International Journal of Robotics and Automation (IJRA)
Vol. 2, No. 4, December 2013, pp. 129~139
ISSN: 2089-4856

Occupancy Grid Mapping Based on DSmT for Dynamic Environment Perception

Zhou Junjing, Duan Jianmin, Yang Guangzu
College of Electronic Information and Control Engineering, Beijing University of Technology

Article Info

Article history:

Received Apr 11, 2013
Revised Jul 23, 2013
Accepted Aug 21, 2013

Keyword:

DSmT
Mobile object detection
Multi-layer laser scanner
Occupancy grid map

ABSTRACT

Occupancy grid mapping is an important approach for intelligent vehicle environment perception. In this paper, an occupancy grid mapping approach in Dezert-Smarandache theory (DSmT) framework for the purpose of dynamic environment perception is proposed. To avoid the transformation of the local map from polar to Catersian coordinate, a different inverse sensor model in Cartesian coordinate for laser scanner was proposed. Two different combination rules in DSmT framework, Dempster's rule of combination and PCR2, are implemented independently for global map update and mobile object detection. The performance of the two combination rules were compared by ways of simulation and experiment. According to the comparisons we find that both of the combination rules are capable of detecting mobile objects. And the former effectively filtered out the noise and make the detection robust, but the latter didn't, suggesting that the former is more suitable for occupancy grid mapping. Static and mobile objects are extracted from the occupancy grid map using digital image processing technology.

Copyright © 2013 Institute of Advanced Engineering and Science.
All rights reserved.

Corresponding Author:

Zhou Junjing,
College of Electronic Information and Control Engineering,
Beijing University of Technology,
100 Pingleyuan, Chaoyang district, Beijing, 100124, China
Email: zhjunjing_2002@163.com

1. INTRODUCTION

Reliable perception of the environment is crucial for Autonomous Cruise Control, collision warning and path planning of the Intelligent Vehicle. In recent years, more and more researchers percept the driving environment by occupancy grid mapping using lidar [1]-[3] or stereo vision [4] information. The advantages of laser scanner are its large field of view and its high angular and range resolution and accuracy. On the other hand, it is particularly convenient to generate an occupancy map if a laser scanner is used.

The building of occupancy grid map is a probability problem because of the uncertainty of the sensor measurement. The main basic approaches to uncertain reasoning are Bayesian probability theory, fuzzy logic and evidence theory. Bayesian inference is the common background used to cope with errors and uncertainty. From the proposal of occupancy grid by Elfes [5] to its successful application in Simultaneous Localization and Mapping (SLAM) [1], Bayesian method rules the greatest part of the work related to the probabilistic sensor fusion.

There have been a lot of researches on occupancy grid mapping in static environment perception. In a structured static environment, all the three methods provide suitable occupancy grid maps [6]. An essential part of the perception problem is the detection of mobile objects because they constitute the more difficult part of the problem when using lidar technology [7]. In recent years, more and more researchers detect mobile objects by occupancy grid mapping. In [3], [8] and [9], the occupancy grid maps are built in Bayesian framework, and the mobile objects are detected by comparing the local map built by current data set and the

accumulated occupancy grid map. R. Alpes et al [10] estimated the occupation and speed of the cells simultaneously by Bayesian Occupancy Filtering (BOF).

As evidence theory can provide conflict analysis for different information sources, and there exist contradictions in the occupancy state of the grid cell caused by moving objects, evidence theory shows excellent capability in moving object detection compared with other approaches. J. Moras et al [7], [11] computed the occupancy grid by DST (Dempster-Shafer theory) evidence framework. There has been much critics on DST for sometimes it results in some abnormal results. So, in recent years, Smarandache and Dezert et al. [12] developed DSmT (Dezert-Smarandache theory) which is an extension of DST to overcome the inherent limitations of it.

In this paper, we present an occupancy grid mapping for environment perception of intelligent vehicles based on DSmT framework. An IBEO LUX laser scanner which has four layers is used to get range information of the environment. As the global grid map and the range information acquitted by the laser scanner are both in Cartesian coordinate, we proposed a different inverse sensor model in Cartesian coordinate to generate local occupancy grid maps, which makes the fusion of the local and global maps more convenient. Two different combination rules in DSmT framework, Dempster's rule of combination and PCR2, are used independently for global map update and mobile object detection. The main purpose of this paper is to compare the performance of these two combination rules in occupancy grid mapping.

This manuscript is organized as follows. Section 2 introduces the occupancy grid mapping and the how is it represented in DSmT framework. Section 3 describes the novel inverse sensor model we built for laser scanner and the building of the local map by the inverse sensor model. Section 4 dedicates in comparing the two different combination rules by simulation and experiments, and extracts objects in the map built by Dempster's rule of combination by DIP technologies. Finally, section 6 concludes the paper.

2. EVIDENTIAL OCCUPANCY GRID MAP

2.1. Representation of Occupancy Grid Map

Occupancy grid is established to represent the map of the environment as an evenly spaced field of binary random variables each representing the presence of an obstacle at that location. Occupancy grid mapping algorithms implement approximate posterior estimation for those random variables. Establishing the occupancy grid map includes three main steps: (1) calculating the inverse sensor model, which specifies the probability that a grid cell is occupied on the base of a single sensor measurement z_t at location x_t. The sensor model we used will be introduced in section 3. (2) mapping the cell state calculated in inverse sensor model into the global map from the sensor reference frame.(3)estimating the posterior probability of occupancy $P(m|x_{1:t}, z_{1:t})$ for each cell m of global grid map M given observations $z_{1:t} = \{z_1, \dots, z_t\}$ at corresponding known poses $x_{1:t} = \{x_1, \dots, x_t\}$. Where, estimation of the occupancy state for each cell by fusing the current sensor observation and the a priori state of the grid map is a conditional probability problem. By using probability methods, the uncertainty brought by the sensor and the position estimation of the mobile robot can be better treated. In this paper, the pose of the mobile robot is supposed to be known and localization is not considered.

2.2. An Evidential Framework for Occupancy Grid Map

In this paper, DSmT is used to incrementally build grid maps of the surrounding environment of the ego vehicle. The development of the DSmT arises from the necessity to overcome the inherent limitations of the DST, one of which is that there will be abnormal fusion results when there exists full contradiction between different information sources to be fused. DSmT can be considered as an extension of the classical DS theory but includes fundamental differences with DST [12].

In occupancy grid map, the cells have two possible states: free and occupied, which are exclusive. So we applied the classical Shafer model which has exhaustive and exclusive elementary hypotheses. It is considered as an example of hybrid DSm models. Specifically, the occupancy grid map based on Shafer model can be described as:

Every cell of the grid map is assigned a state between two possible values Free (F) and Occupied (O). The power set is defined as 2^{Ω}= {F, O, Ω,Φ, }. Where Ω represents the ignorance state F∪O, andΦ represents the conflict information F∩O. For each cell, a mass function is calculated and provides four beliefs on the state of the cell [m(F) m(O) m(Ω)m(Φ)], where m(A) represents respectively the piece of evidence that the space is free, occupied, unknown or resulting of conflict. Mass functions verify the property $\sum_{A\subseteq\Omega} m(A) = 1$.

To present the surrounding environment of the intelligent vehicle, two grid maps have to be built: a local map ScanGrid (SG) for the capture of the sensor information and a global map MapGrid (MG) for the temporal integration of data in a fixed frame [13].

3. BUILDING THE SCANGRID

Commonly, the inverse sensor model is built in polar frame but the MapGrid is in Cartesian reference frame [13**Error! Bookmark not defined.**],[14]. Before fusion of the local and global map, bi-linear interpolation method has to be adopted to convert the ScanGrid from polar to Cartesian coordinates. The transformation will not only increase the computation consumption but also increase the false alarms on static objects [13]. Therefore, we build the sensor model in Cartesian coordinate so that the two maps are compatible and the transformation of the SG from polar to Cartesian coordinate is avoided.

The IBEO LUX laser scanner which has four scan layers is shown in Figure 1. The lidar can reach a distance of 200m with a 110° angular aperture. The angel solutions are 0.125°, 0.25° and 0.5° differing by sector as shown in Figure 2. The data point got by the sensor is presented as [x, y, z, r], where [x, y, z] is the coordinate values and [r] is the distance of the point to the sensor. The position of the laser scanner is set to be the origin of the Cartesian coordinate, the travel direction of the ego vehicle is defined as the x-axis and the direction vertical to the ground is defined as the z-axis. The data reflected from the ground are omitted in our model, in other words, the useful data are all from obstacles. In order to avoid huge calculation processes, we assume that the cells are independent to each other [15].

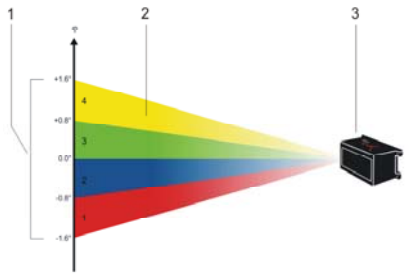

Figure 1. IBEO LUX laser scanner (1 vertical opening angle 2 Scan level 3 IBEO LUX)

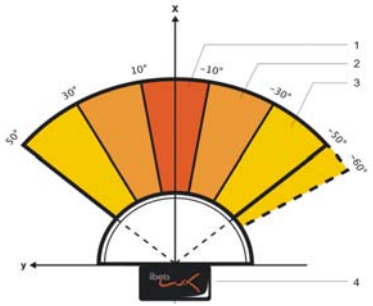

Figure 2. Angle resolutions differing by sector

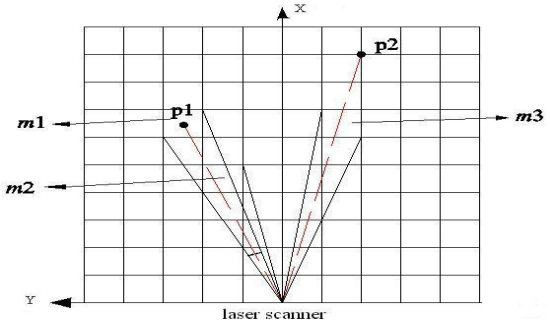

Figure 3. Inverse sensor model (p1 and p2 are two data points obtained by the sensor, m1, m2 and m3 are three different cells)

The space is divided by $m \times n$ cells with a size of $l \times l$ as shown in Figure 3. Each cell is presented by three variables: the first one describes the position of the cell center in Cartesian coordinate, presented as [x_m , y_m ,]. The second one describes the angel scale [θ^- , θ^+] of the cell, where, θ^- and θ^+ represent the lower and upper angle limits of the cell respect to the sensor. And the third one is the distance d from the cell center to the sensor. The first variable is used to fuse the ScanGrid with the MapGrid, and the last two variables are used to determine the cell state of ScanGrid by projecting the sensor data.

The measurement set projected in cell m is:

$$P=\left\{ p_i=\left[x_i,\quad y_i,\quad z_i,\quad r_i\right].\arctan\frac{y_i}{x_i}\in\left[\theta_m^{-},\theta_m^{+}\right],i\in\left[1,n\right]\right\}$$

For each cell *m*, the cell state is determined by the following principle:

- $\forall i\in\left[1,n\right]$ if $\exists r_i \mid r_i\in\left[d-l/2,d+l/2\right]$ then the cell state is occupied.

- $\forall i\in\left[1,n\right]$ if $\nexists r_i \mid r_i\in\left[d-l/2,d+l/2\right]$ and $d+l/2<\min\left(r_i\right)$, then the cell state is free.

- $\forall i\in\left[1,n\right]$ if $\nexists r_i \mid r_i\in\left[d-l/2,d+l/2\right]$ and $d-l/2>\min\left(r_i\right)$, then the cell state is unknown.

The cells out of the scan scale of the laser are defined to be unknown.

The mass functions for different cell states are defined by formula (1):

$$\begin{cases} free: m\left(F\right)=1-\lambda_{md}, m\left(O\right)=0, m\left(\Omega\right)=\lambda_{md} \\ occupied: m\left(F\right)=0, m\left(O\right)=1-\lambda_{fa}, m\left(\Omega\right)=\lambda_{fa} \\ unknown: m\left(F\right)=0, m\left(O\right)=0, m\left(\Omega\right)=1 \end{cases} \quad (1)$$

Where, λ_{md} and λ_{fa} are the miss detection rate and false alarm rate separately. According to the upper principle, cell m1 in Figure 2 is occupied, m2 and m3 are free.

When a new ScanGrid is built, the fusion of it with the MapGrid could be executed by shift and rotate transformation in the same coordinate system and the transformation from polar to Cartesian coordinate is avoided.

4. DATA FUSION AND MOVING OBJECT DETECTION

4.1. Analysis on the MapGrid Update Process

Starting with an initial map, the robot successively extends the map by incorporating local maps generated in Section 3. The problem we face now is how to combine the mass function of m_t^{SG} in SG at time t and the a priori mass function of m_{t-1}^{MG} in MG at time t-1when new data arrive. In this paper, two different combination rules are implemented independently in the fusion process: Dempster's rule of combination and PCR2. Dempster's rule of combination is the most widely used rule of combination so far in many expert systems based on belief functions since historically it was proposed by Shafer. It abandons the conflict information and takes a normalization procedure to all the non-empty sets. In DSmT, the conflict information is redistributed proportionally on non-empty sets by some rules (PCR1-PCR5). In this paper we take PCR2 as a representation which is relatively simple.

Here we instantiate the fusion process taking one grid cell for example by simulation. In the simulation, the sensor observation of the cell is divided into 3 stages: free (time step 0-9), occupied (time step 10-29) and free (time step 30-50) as shown in Figure 4(a). The initial state of the corresponding cell in MapGrid is unknown. The mass functions are defined by formula (1), and $\lambda_{md}=\lambda_{fa}$=0.2.

4.1.1. Fusion by Dempster's rule of combination

Both Dempster's rule of combination and PCR2 are based on the conjunctive rule. The conjunctive rule in Shafter model with 2 sources is defined as:

$$m_{1,2}\left(A\right)=\sum_{\substack{X_1,X_2\in 2^{\Omega}\\ X_1\cap X_2=A\neq\Phi}} m_1\left(X_1\right)m_2\left(X_2\right) \quad (2)$$

The Dempster's rule of combination is specified as:

$$m_{DS}\left(\Phi\right)=0 \quad (3)$$

$$m_{DS}(A) = \frac{m_{1,2}(A)}{1-K} \tag{4}$$

$$K = \sum_{\substack{X_1, X_2 \in 2^{\Omega} \\ X_1 \cap X_2 = \Phi}} m_1(X_1) m_2(X_2) \tag{5}$$

Where, K is a measure of the amount of conflict between the two sources. In this paper, we maintain the conflict information for moving object detection.

Fig. 4b shows the fused cell state in MapGrid by Dempster's rule of combination additional with the conflict information. By comparing Figure 4(a) and Figure 4(b), we can find that, at the beginning the cell state of MapGrid converges from Unknown to Free immediately. At time step 10, the sensor observation changed from Free to Occupied, but the fused cell state in MapGrid remains to be Free until time step 19. There is similar response when the sensor observation changes from Occupied to Free at time step 30. That is to say, there is a delay for the MapGrid to converge to be consistent with the sensor observation when the sensor observation changes.

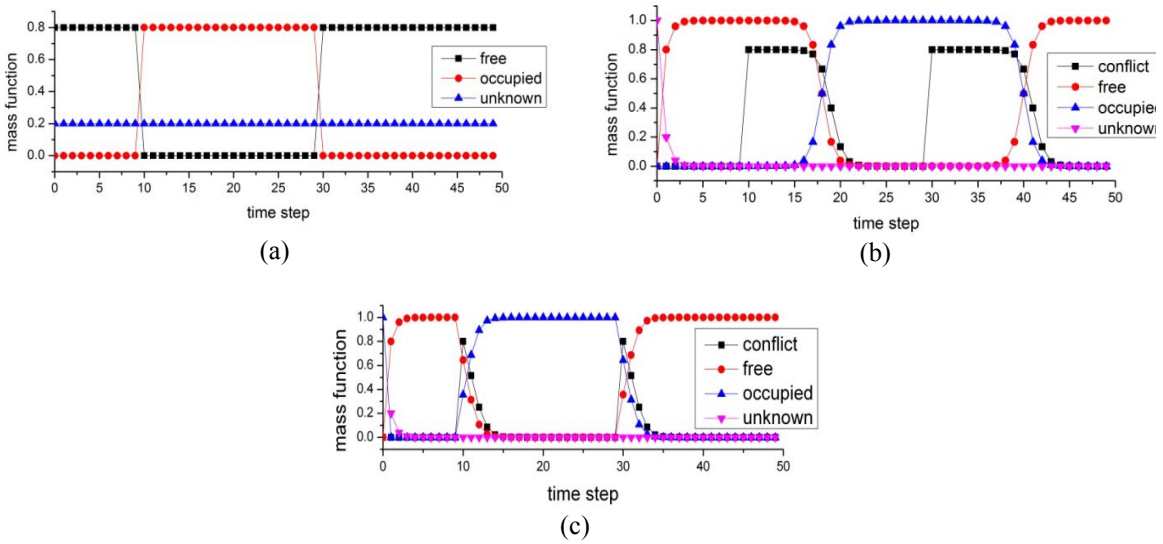

Figure 4. Simulation of the evolution of the mass function(a: evolution of the ScanGrid cell, b: fusion result of the MapGrid cell by Dempster's rule of combination, c: fusion result of the MapGrid cell by PCR2)

4.1.2. Fusion by PCR2

In PCR2, the total conflict information calculated in formula (5) is distributed only to the non-empty sets involved in the conflict (not to all non-empty sets) proportionally with respect to their corresponding non-empty column sum [16].

Figure 4(c) shows the simulation of the evolution of the mass function calculated by PCR2 with the sensor observation shown in Figure 4(a). We can find that the cell state changed immediately along with the sensor observation. The conflict information only appears in the short period during which the MG cell state converges to be the same with the sensor observation. In other words, the redistribution of the total conflict information makes the fusion result closer to the real situation than Dempster's rule of combination does. This proves that PCR rules are theoretically better than Dempster's rule of combination.

To illustrate how PCR2 makes the fusion result more credible than Dempster's rule of combination when there is a change in the sensor observation, we calculate the fusion by the two combination rules at time step 10 of the simulation as following:

Denote the mass functions of m_t^{SG} and m_{t-1}^{MG} as m_1 and m_2. At time step 10, the two mass functions are:

$$m_1(F) = 0.8, m_1(O) = 0, m_1(\Omega) = 0.2$$

$$m_2(F)=1, m_2(O)=0, m_2(\Omega)=0$$

Apply the conjunctive rule in formula (2) and we can get:

$$m_{12}(F)=0.2, m_{12}(O)=0, m_{12}(\Omega)=0$$

According to formula (5), the total conflict information K=0.8.

The fusion by Dempster's rule of combination is described as:

$$m_{DS}(F)=\frac{m_{12}(F)}{1-K}=\frac{0.2}{1-0.8}=1,$$

$$m_{DS}(O)=\frac{m_{12}(O)}{1-K}=\frac{0}{1-0.8}=0,$$

$$m_{DS}(\Omega)=\frac{m_{12}(\Omega)}{1-K}=\frac{0}{1-0.8}=0$$

Denote that $c_{12}(F)=m_1(F)+m_2(F)=1$, $c_{12}(O)=m_1(O)+m_2(O)=0.8$, $e_{12}=c_{12}(F)+c_{12}(O)=1.8$.

The fusion by PCR2 is described as:

$$m_{PCR2}(F)=m_{12}(F)+\frac{c_{12}(F)}{e_{12}}*K=0.2+\frac{1}{1.8}\times 0.8=0.64$$

$$m_{PCR2}(O)=m_{12}(O)+\frac{c_{12}(O)}{e_{12}}*K=\frac{0.8}{1.8}\times 0.8=0.36$$

$$m_{PCR2}(\Omega)=m_{12}(\Omega)=0$$

From the above calculation we can notice that, as the MapGrid shows full knowledge of the cell state ($m_{t-1}^{MG}(F)=1$), even if the sensor observation m_t^{SG} changes to the opposite of the a priori MG cell state m_{t-1}^{MG}, the fusion result by Dempster's rule of combination is still identical with m_{t-1}^{MG}. However, the redistribution of the conflict information brings a relatively reasonable fusion result.

4.2. Moving objects detection

A change in the sensor observation can be caused by either noise or motion [1]. At first, we simulate the moving object detection process. The sensor observation for a grid cell that experiences the process of a moving object passing by is shown in Figure 5(a). Suppose that the object remains in the cell for 3 time steps (with a velocity of about 6km/h, assuming that the frequency of the laser scanner is 12.5Hz and the cell size is 0.4m×0.4m). In grid mapping, conflict information K (formula (5)) consists of two parts: $C1=m_{t-1}^{MG}(F)*m_t^{SG}(O)$ which indicates the conflict induced when a free cell in MG is fused with an occupied cell in SG, and $C2=m_{t-1}^{MG}(O)*m_t^{SG}(F)$ which indicates the conflict induced when an occupied cell in MG is fused with a free cell in SG. In this paper, we consider the two parts separately. Theoretically, the direction of moving objects can be detected by these two parts of the conflict information (from C2 to C1) [7].

Figure 5(b) shows the simulation of the evolution of the MG cell when a moving object passes through by implementing Dempster's rule of combination. It was found that the fused cell state kept to be free (m(O)=0) throughout the whole process. This situation is consistent with that in Figure 4(b), indicating that the MG cell state will not change in a short time when the sensor observation changes. After the object has moved out of the cell, the conflict information C2 is zero due to the delay of the cell state. Fortunately, the conflict information C1 is so high to detect the moving object easily although the cell state doesn't change. The direction of the moving objects however fails to be recognized due to the absence of the conflict information C2. Object tracking algorithm has to be adopted to determine the direction and velocity of moving objects.

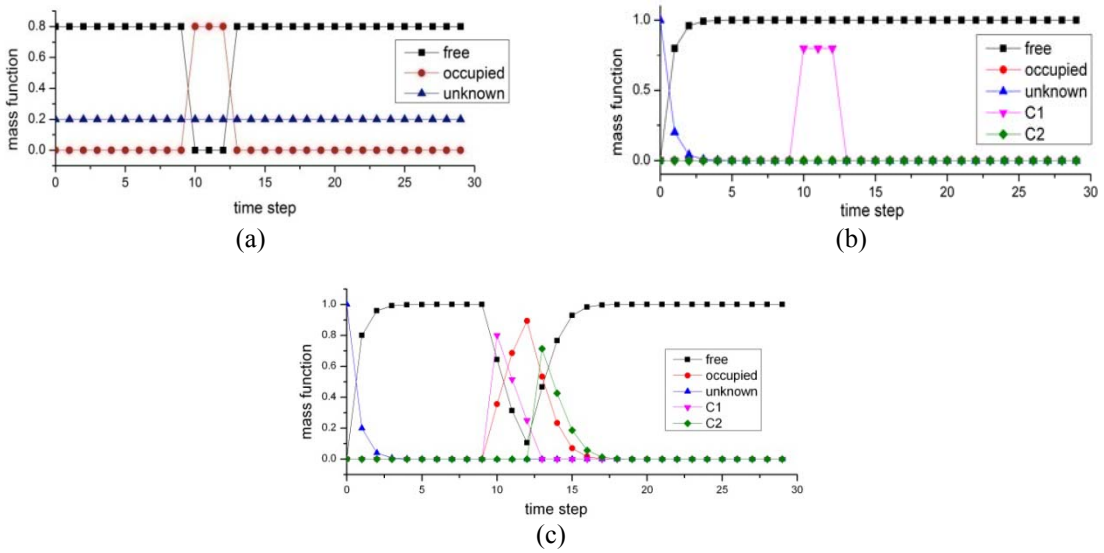

Figure 5. Evolution of the cell state as an object passing through a cell(evolution of the ScanGrid cell, b: fusion result of the MapGrid cell by Dempster's rule of combination, c: fusion result of the MapGrid cell by PCR2)

Figure 5(c) shows the moving object detection result by implementing PCR2. The MG cell state changes to be occupied at the second time step after the cell is occupied. And both C1 and C2 are presented obviously. That is to say, the direction of the moving object could be recognized by implementing PCR2. This theoretically proves again the advances of PCR rules with respect to Dempster's rule of combination.

From the above simulations, we can conclude that both Dempster's rule of combination and PCR2 can detect mobile objects directly during the MapGrid update procedure. We think this advantage owes to the fact that evidence theory has the ability to come up with the probability of a collection hypotheses, which is an important merit compared with Bayesian probability theory. In Bayesian framework, after fusion of the ScanGrid and MapGrid, extra work of comparing the two kinds of maps has to be done to detect moving objects [3], [8].

4.3. Static Objects Detection

Suppose that a grid cell is occupied by static object, and there exist noise in the sensor measurement. Here we suppose the cell state kept to be free for 3 time steps as a measurement noise. The evolution of the ScanGrid cell state is shown in Figure 6(a).

Figure 6(b) shows the corresponding cell state in MapGrid calculated by Dempster's rule of combination. The result is similar to that of a moving object passes through a free space shown in Figure 5(b). Different with the mobile object detection, in static object detection, although the conflict information C2 appears when there is noise, as the cell state keeps to be occupied, we can regard the cell as occupied and take no account of the conflict information. Thus the noise is filtered out and the detection for static objects is robust.

Figure 6(c) illustrates the cell state calculated by PCR2. As the cell state changes along with the sensor measurement, the noise will appear apparently in the cell.

4.4. Object Extraction

Some of the environment perception algorithm based on occupancy grid mapping extracts objects from the raw sensor data after building the grid map [9]. In this paper, objects were extracted from the grid cells, so that there is no assumption on the shape of the objects, making it suitable for a wide range of urban objects (pedestrians, vehicles, bicycles …).

The evidence grid map can be seen as a double channel image: one channel indicates if the cell is occupied and the other does if the cell is mobile. We use several digital image processing approaches in object extraction step. Due to the discontinuity of the raw sensor data, sometimes the cells belonging to one object do not connect to each other. We implemented dilation and erosion operation to connect the nearby cells and repair the holes in an object. Dilation and erosion are two fundamental morphological operations. Dilation followed by erosion is called closing operation which can smooth the contours, fuse narrow breaks and long thin gulfs, eliminate small holes, and fill gaps in the contours of an image. Here we use a 3×3

structuring element to do the dilation and erosion operation. By using the closing operation, split objects will be merged. Then a connected components analysis is implemented and the connected cells were labeled. Cells with the same label are seen as an object.

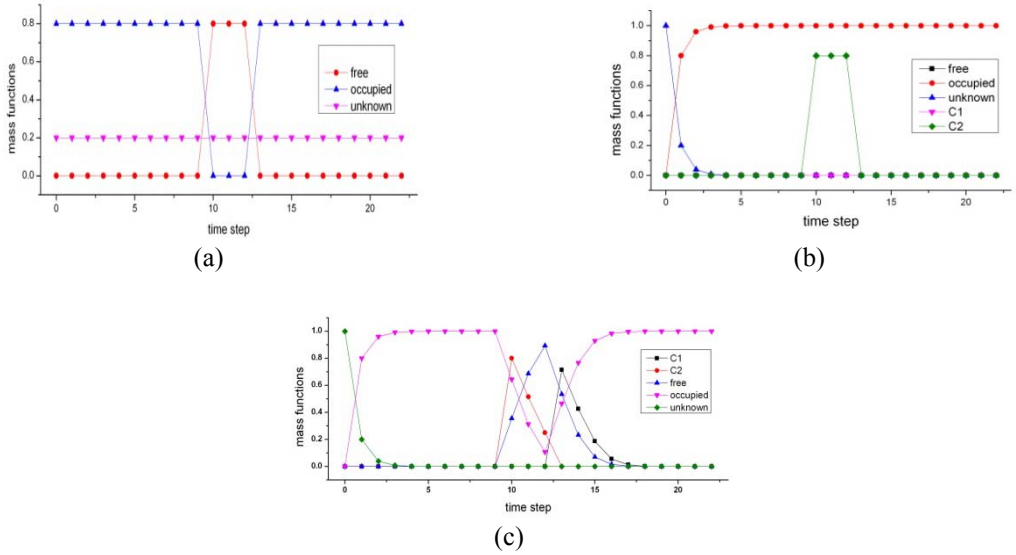

Figure 6. Evolution of the state of an occupied cell disturbed by noise(evolution of the ScanGrid cell, b: fusion result of the MapGrid cell by Dempster's rule of combination, c: fusion result of the MapGrid cell by PCR2)

4.5. Experiment Results

The two different combination rules were tested on a dataset acquired with the vehicle BJUT-IV equipped with an IBEO LUX laser scanner in the campus of BJUT. The lidar frequency was 12.5Hz. The video was recorded simultaneously for validation and visualization of the scene.

The cell size in both ScanGrid and MapGrid is 0.4m×0.4m. and the ScanGrid covers a field of 80m×32m. The miss detection rate λ_{md} and false alarm rate λ_{fa} are set to be 0.2. If the value of conflict information C1≥0.1, the cell is considered to be occupied by mobile object. If the value of conflict information C2≥0.1, the cell is considered to be the past position of a mobile object.

Figure 7 and Figure 8 show the results of two different scenes. In scene Ⅰ (Figure 7), objects 1 and 2 are mobile, and object 3 is static. In scene Ⅱ (Figure 8), objects 1,2 and 3 are all mobile. In each scene, the ScanGrid generated by the inverse sensor model, the fusion results by PCR2 and Dempster's rule of combination, and the object extraction results are shown. The objects were manually framed with the same color on the camera snapshot and on the maps in order to identify them.

4.5.1. ScanGrid generated by the Cartesian sensor model

Figure 7(b) and Figure 8(b) show the ScanGrid maps generated by the inverse sensor model. Green indicates occupied state, white indicates free and grey indicates unknown. The dots with different colors in the occupied cells are data points in different layers. From the figure we can find that the sensor data was well transformed into an occupancy map by the inverse sensor model. The following MapGrid update process can be executed directly by fusing this ScanGrid map.

4.5.2. MapGrid update and moving object detection result

Figure 7(c) and Figure 8(c) show the MG updated by PCR2, and Figure 7(d) and Figure 8(d) show the MG updated by Dempster's rule of combination. Green indicates static object, red indicates conflict information C1, blue indicates conflict information C2, and white indicates free space.

From the figures we can find that,

1) In mobile objects detection, the conflict information C1 can be presented by both combination rules (red cells in Figure 7(c)-(d) and Figure 8(c)-(d). C2 only appears in the MapGrid calculated by PCR2 (Figure 7(c) and Figure 8(c). When we use Dempster's rule of combination for MapGrid update, as the

mobile object doesn't remain enough time on the cells to change the cell state, the conflict information C2 doesn't appear (Figure 7(d) and Figure 8(d). This result verifies the simulation analysis in section 4.2.

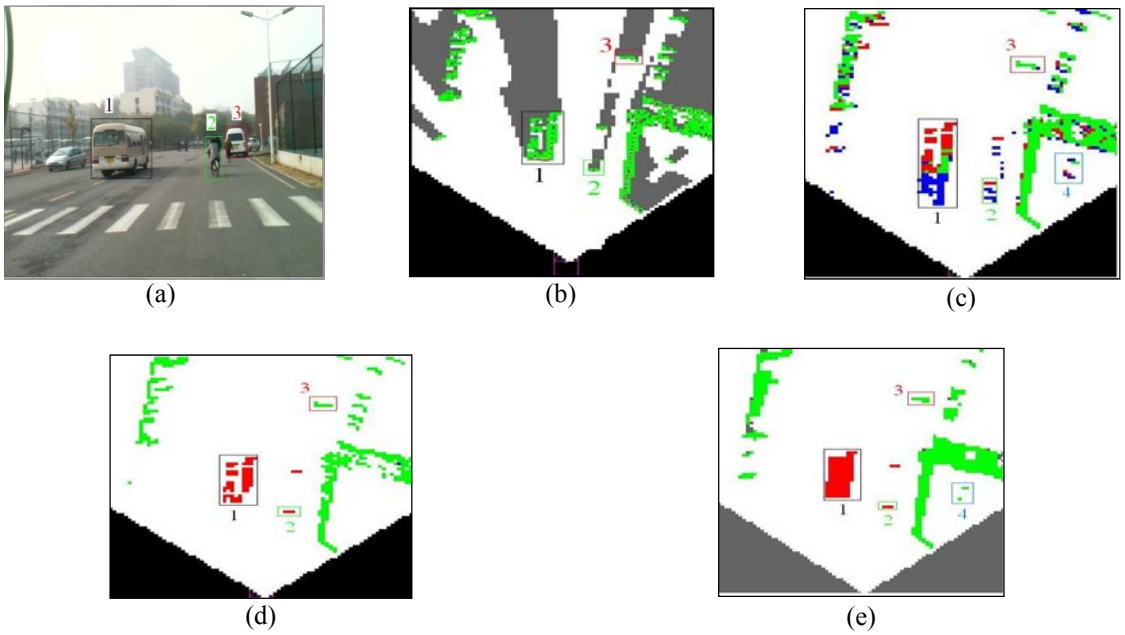

(a) (b) (c) (d) (e)

Figure 7. Environment perception result of scene Ⅰ (a: the snapshot of the scene, b: the ScanGrid map, c: the fused MG by PCR2, d: the fused MG by Dempster's rule of combination, e: object extraction by digital image process technology)

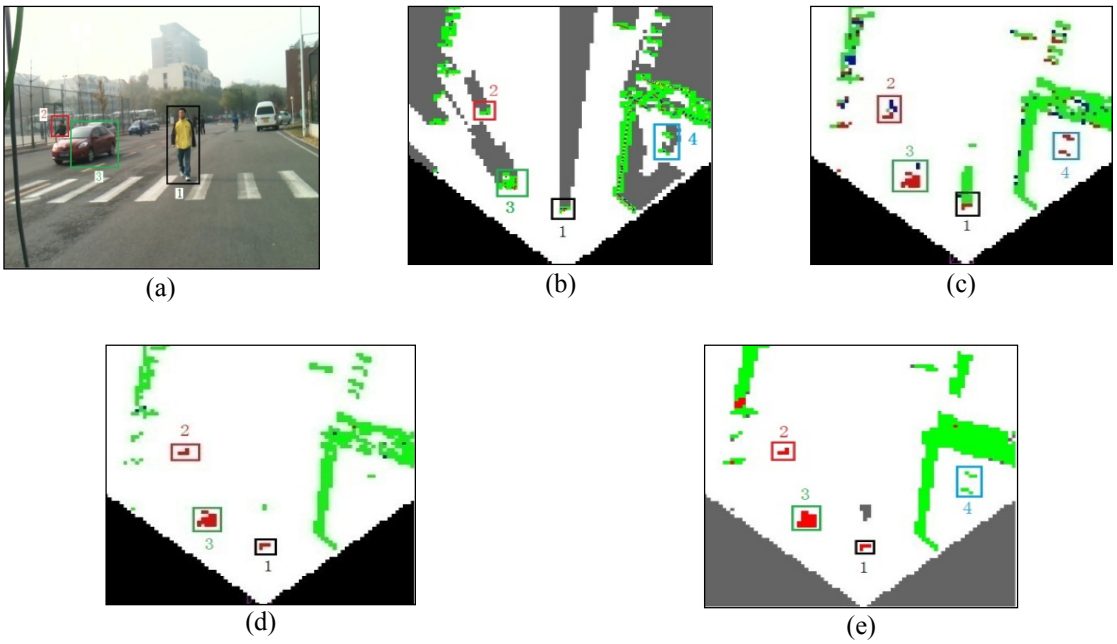

(a) (b) (c) (d) (e)

Figure 8. Environment perception result of scene II. (a: the snapshot of the scene, b: the ScanGrid, c the fused MG by PCR2, d: the fused MG by Dempster's rule of combination, e: object extraction by digital image process technology)

2) In static objects detection, there are many mobile cells scattered on the static objects in the MapGrid calculated by PCR2. This phenomenon is due to the measurement noise. But Dempster's rule of combination could filter out the noise and makes the static object detection stable. This verifies the analysis in section 4.3. Another kind of measurement noise is occupied cells on free space (object 4 in Figure 7 and

Figure 8, it can't be seen in the photos). This kind of noise appears alternately by time steps. When we use PCR2, as the cell state changes immediately along the measurement, the noise will be presented as a mobile object (Figure 7(c) and Figure 8(c)), and this will cause false alarm. But in the MG calculated by Dempster's rule of combination (Figure 7(d) and Figure 8(d)), the noise is filtered out or appears as static objects.

3) The minibus (object1 in Figure 7(d)) is in pieces and it's inconvenient for object detection and tracking. We implemented closing operation and connected components analysis on the MapGrid generated by Dempster's rule of combination. We can see that the minibus is connected to a single object from pieces in Figure 7(e). The nearby static objects on the roadside are also connected. The connection of the minibus will make the mobile object tracking more efficient. There is no negative effect if the adjacent static or mobile objects were connected to a whole one.

5. CONCLUSION

In this paper we have proposed an occupancy grid framework based on DSmT. We built the inverse sensor model in Cartesian reference frame so that the transformation from polar to Cartesian coordinate is avoided. The performance of Dempster's rule of combination and PCR2 in building the occupancy grid maps are compared by simulation and experiment. From the analysis we conclude that:

1) Dempster's rule of combination is adoptable for occupancy grid mapping. In the definition of the mass functions of the sensor model in formula (1), false alarm rate λ_{fa} and miss detection rate λ_{md} are introduced, i.e. there is a discounting on the reliability of the evidence. So the conflict information K is always less than 1 and the denominator (1-K) in formula (4) will never equal to zero. There is no abnormal result caused by full confliction during occupancy grid map update.

2) Both of the approaches are capable of detecting moving objects. But the direction of moving objects can't be detected by Dempster's rule of combination as the conflict information C2 doesn't appear. This result is different with that from [7] which indicates that both C1 and C2 could be presented by Dempster's rule of combination.

3) In static objects detection, Dempster's rule of combination is more robust than PCR2 as the former can efficiently filter out the measurement noise. If we use Dempster's rule of combination, due to the delay of the cell state of MapGrid when the sensor measurement changes, the noise doesn't appear. This makes the static object detection more stable and decreases the false alarm rate. But by PCR2, the cell state will change immediately when the sensor observation changes. So the noise information will be totally presented.

Considering the above analysis, we think that the classic Dempster's rule of combination is more suitable than conflict information redistribution rules in occupancy grid mapping, though the combination results by the latter is more reasonable than that by the former. So we applied closing operation and connected components analysis on the MapGrid generated by Dempster's rule of combination. This map will be adopted in our future works of mobile objects tracking and path planning.

REFERENCES

[1] Petrovskaya S Thrun. Model based vehicle detection and tracking for Autonomous Urban Driving. *Autonomous Robots.* 2009; *26*: 123-139.
[2] T Weiss, B Schiele, K Dietmayer. Robust Driving Path Detection in Urban and Highway Scenarios Using a Laser Scanner and Online Occupancy Grids. *IEEE Intelligent Vehicle Symposium.* 2007: 184-189.
[3] S Pietzsch, TD Vu, J Burlet, et al. Results of Precrash Application Based on Laser Scanner and Short-Range Radars. *IEEE Transactions on intelligent transportation systems.* 2009; *10:* 584-593.
[4] Radu Gabriel Danescu, Cluj-Napoca. Obstacle Detection Using Dynamic Particle-Based Occupancy Grids. *International Conference on Digital Image Computing: Techniques and Applications.* 2011: 585-590.
[5] A Elfes. Using occupancy grids for mobile robot perception and navigation. *Computer.* 1989; *22:* 46-57.
[6] M Ribo, A Pinz. A comparison of three uncertainty calculi for building sonar-based occupancy grids. *Robotics and Autonomous Systems.* 2001; *35:* 201-209.
[7] J Moras, V Cherfaoui, P Bonnifait. Moving objects detection by conflict analysis in Evidential Grids. *IEEE Intelligent Vehicle Symposium.* 2011: 1122-1127.
[8] A Azim, O Aycard. Detection Classification and Tracking of Moving Objects in a 3D Environment. *Intelligent Vehicle Symposium*. 2012; 802-807.
[9] ME Bouzouraa, U Hofmann. Fusion of Occupancy Grid Mapping and Model based Object Tracking for Driver Assistance Systems using Laser and Radar Sensor. *IEEE Intelligent Vehicle Symposium. 2010:* 294-300.
[10] R Alpes, G CNRS. Bayesian Occupancy Filtering for Multitarget Tracking: An Automotive Application. *International Journal of Robotics Research.* 2006; *25:* 19-30.

[11] J Moras, SA Rodriguea F, V Drevelle, et al. Drivable Space Characterization using Automotive Lidar and Georeferenced Map Information. *IEEE Intelligent Vehicle Symposium*. 2012: 778-783.
[12] F Smarandache, J Dezert. Advances and Applications of DSmT for Information Fusion (Collected Works). Rehoboth: American Research Press. 2004.
[13] J Moras, V Cherfaoui, P Bonnifait. Credibilist Occupancy Grids for Vehicle Perception in Dynamic Environments. *IEEE International Conference on Robotics and Automation*. 2011; 84-89.
[14] S Thrun, W Burgard, D Fox. Probabilistic Robotics. Cambridge, USA: MIT Press. 2005: 281-301.
[15] A Elfes. Occupancy Grids: A probabilistic framework for robot perception and navigation. Carnegie-Mellon University. 1989.
[16] F Smarandache, J Dezert. Advances and Applications of DSmT for Information Fusion (Collected Works). Rehoboth: American Research Press. 2006.